



# The uniaxial compressive strength of concrete: revisited

David Z. Yankelevsky 

Received: 17 February 2024 / Accepted: 30 June 2024 / Published online: 12 July 2024  
© The Author(s) 2024

**Abstract** This paper re-examines common notions and conventions regarding the compressive strength of concrete in general and of the uniaxial compressive strength of concrete in particular. A distinction is introduced between the strength of the specimen and the strength of the concrete as a material, and the commonly measured and adopted strength is shown to be the specimen's strength, wrongly interpreted as the material's strength. The two major damage modes of concrete specimens (with the formation of either longitudinal cracks or shear bands) are discussed. Such failure modes are wrongly considered as features of concrete behavior in uniaxial compression, but this is not the case. Longitudinal cracking is due to lateral expansion (Poisson's effect) and occurs at a relatively low applied load in absence of friction at specimen's top and bottom boundaries. Shear failure (accompanied by the formation of an inclined shear band) is related to the shear envelope parameters that are related to the concrete mixture, but the applied ultimate pressure is not the concrete uniaxial compressive strength. Hence, though caused by applied compressive loading, these failure modes are little/hardly related to the concrete material intended as the ultimate uniaxial stress (strength) corresponding to a

maximum value of the uniaxial compressive strain. Using the shear envelope parameters has been proven to yield a very good prediction of the applied compressive loading of the specimen in the limit state, as a demonstration that the applied pressure at specimen's failure resulting from the formation of inclined fracture bands is the specimen's failure strength, and not the material's compressive strength! Reasons are given against the existence of a uniaxial compressive strength failure for concrete, and a piece of evidence in this direction is provided by concrete specimens subjected to pure hydrostatic compression, that do not fail at all. The entire issue requires, therefore, a deep revisiting and re-thinking, to provide correct measures for representing concrete response under compression in analysis and design.

**Keywords** Concrete compressive strength · Specimen compressive strength · Concrete · Standard testing · Cracking · Shear failure · Shear envelope · Friction

## 1 Introduction

### 1.1 General

The uniaxial compressive strength of concrete, or as it is commonly known “the compressive strength of concrete”, is the most basic concrete property and is the most commonly used term in concrete mechanics.

---

D. Z. Yankelevsky (✉)  
National Building Research Institute, Faculty of Civil  
and Environmental Engineering, Technion-Israel Institute  
of Technology, 32000 Haifa, Israel  
e-mail: davidyri@technion.ac.il



It is mentioned in every document on concrete structures, and numerous books dedicate chapters to describe the behavior of concrete under compressive stresses with emphasis on its uniaxial compressive strength [1, 2]. All relevant standards, manuals and model codes [3–6] refer to the compressive strength of concrete as the key parameter that also determines other important related parameters of concrete, such as the tensile strength, shear strength, bond strength, Young's modulus of elasticity etc. The Model Code [6] states that “concrete is classified on the basis of its compressive strength. Design is based on a grade of concrete” which is measured in simple standard tests referring on standard size cubes or cylindrical specimens [6–8]. The standard specimens are cast in special molds, and undergo a specified curing procedure. At a standard age of 28 days, the specimen is placed in a test apparatus and it is tested under uniaxial compressive pressure loading. In the case of a cube specimen, pressure is applied through top and bottom steel platens. A gradually increasing compressive loading is commonly applied by a displacement controlled loading procedure. Loading continues until damage appears and it extends until specimen failure occurs. The maximum compressive pressure loading applied on the specimen is interpreted as the concrete uniaxial compressive strength. Due to the concrete material heterogeneity, different specimens exhibit somewhat different strength results, therefore a sample of several specimens is required to determine the average uniaxial compressive strength. Adding displacement transducers like LVDT (Linear Variable Differential Transformer) to measure the longitudinal shortening of the specimen during a test, provides the load–displacement relationship of the specimen in the longitudinal direction and it is converted to the average stress–strain relationship of concrete in uniaxial compression (Fig. 1). This continuous curve is not required for the strength determination, however it provides insight into the specimen behavior under compressive loading and is widely used in structural analysis to represent the concrete constitutive behavior.

The ascending branch starts with a linear force–displacement relationship which characterizes the specimen's loading almost up to the maximum load level. Early damage is observed close to the peak load, thus affecting the slightly curved upper part of the ascending branch with increasing displacement.

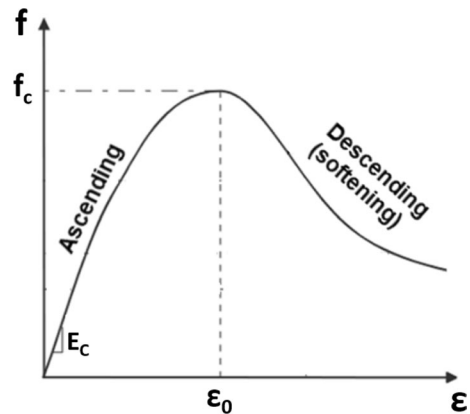


**Fig. 1** A typical uniaxial compressive stress–strain curve

The peak stress in the stress–strain curve is denoted the compressive strength of concrete  $f_c$  (Fig. 1).

Beyond the peak load level, the continuing specimen's response exhibits a nonlinear behavior with stiffness reduction showing the descending (softening) behavior of the specimen associated with increasing damage until failure, and is known as the softening behavior of concrete in compression.

The present paper focuses on the uniaxial compressive strength aiming at clarifying its nature and significance.

## 1.2 Parameters affecting the maximum compressive load resisted by the specimen

For a given concrete type, the maximum a uniaxial compression load may be applied on a specimen until its failure, which depends on numerous parameters, such as the specimen shape (cube, prism or cylinder) and size, its aspect ratio, loading parameters (e.g., loading rate, force/displacement control loading), specimen confinement, boundary conditions, etc. The effects of the different parameters on the specimen response to the compressive axial loading have been a subject of extensive research [9, 10]. In an attempt to develop a standard test method for measuring the complete stress–strain curve, including the softening part, an extensive round robin test program was carried out by a group of laboratories and their findings are described in a comprehensive paper [11]. The main examined variables were the concrete strength (NSC or HSC), specimen shape and slenderness, and the boundary

restraint caused by the friction of the loading platens and by its reduction using different techniques. It was confirmed that using rigid steel platens yields an apparent compressive strength, or, in fact, an applied compressive pressure, of higher magnitude with decreasing specimen slenderness; this apparent strength dependence on the slenderness is not observed when lubricated platens are used and a rather constant strength is measured independent of the specimen slenderness. The dependence on slenderness in the case of common steel platens is explained by the formation of a triaxial state of stress in the specimen contact zones with the platens due to friction developed between the steel platens and the specimen top and bottom faces. This 3D state of stress zone, covers most of the specimen height in low slenderness specimens, thus forming a hour-glass failure mode, whereas longitudinal cracks parallel to the specimen's axis and loading direction are observed along the central part of a specimen with higher slenderness. Such longitudinal cracks are also observed in low slenderness commonly used specimens that are loaded with reduced friction platens. Thus, the magnitude of the maximum applied pressure at failure, and the mode of damage depend on the boundary conditions. This annoying effect sheds doubt on the quality and meaning of the test results.

The obtained stress–strain curve shape also depends on the boundary conditions: in the case of low friction, the stress–strain curve is characterized by a limited post peak zone (i.e., a sharp descent of the softening branch). The applied peak pressure in the case of low friction, is considerably lower (even by 40–50%) than the peak pressure obtained in the case of regular steel platens. Different techniques were examined to reduce platens friction, including a single/several Teflon sheet/s, different Teflon sheet thickness, a set of two Teflon sheets with a thin grease layer in between, talk powder, synthetic rubber layers, etc. It is interesting to note that different friction reduction techniques yielded different stress–strain curves mainly affecting the magnitude of the peak compressive strength and the shape of the softening branch. Document [11] stated that under different conditions, the apparent strength may be higher or lower than “the true compressive strength, (whatever that may be)”. This saying indicates that the true compressive strength is unknown, and that the

referred study focuses mainly on the relative effects of the different variables.

Although document [11] is rich with experimental details, its conclusions provide some fuzzy messages. For example, stating that “the strength of concrete is dependent on the type of loading platen used and the slenderness of the specimen” involves test conditions with material properties and indicates that the true material property cannot be determined.

In another paper [12], a section is dedicated to the question: “Standard test for uniaxial compression?”. The author states that for specimens slenderness 2:1, the complete stress–strain curves show relatively narrow scatter where Teflon layers are used to reduce friction of the steel platens. The author declares that using that friction reduction method means that “*the strength of the material approaches the lower asymptote, which is associated with the uniaxial compressive strength*”. That statement means that lesser friction approaches the “real” compressive strength of concrete, whatever it is. A recommended setup is presented in [12] implementing a friction reducing system that is composed of two 100  $\mu\text{m}$  Teflon layers with a 50  $\mu\text{m}$  grease layer in between. That recommendation appears in Rilem TC-148-SSC document [13] as the recommended test method for measurement of the strain-softening behavior of concrete under uniaxial compression. This recommended standard test setup method is supposed to decrease the scatter of results and yield a relatively lower magnitude of the maximum compressive loading and a shorter strain span of the softening branch.

The present paper claims that it is not clear at all why approaching the lower asymptote, namely towards loading with no associated friction, approaches the uniaxial compressive strength, and wonders whether the reduced friction test is indeed the right test to determine the compressive strength of concrete. That question will be examined in detail in the following.

The Rilem TC-148-SSC document [13] aims at summarizing the state of knowledge that leads to the above recommendation. It refers to the strain softening as the loss of compression load carrying capacity and focuses on the softening branch which is considered an important part of the complete stress–strain diagram of the concrete uniaxial compression behavior, that is essential for structural analysis. These statements tightly relate Fig. 1

to the overall behavior of concrete under uniaxial compression, and its peak stress as the uniaxial compressive strength of concrete. This paper casts doubts on the correctness of these statements.

The above introduction presents in a nutshell some of the complexity involved in the subject under discussion. The findings are confusing and require further investigation. Although much data and many observations have been accumulated, they evoke many questions, several of which have been mentioned above. The unavoidable pronounced question, is: what is really the compressive strength of concrete?.

### 1.3 Objectives and research approach

This paper aims at carefully examining several major aspects regarding the uniaxial compressive loading of a concrete specimen and its relationship to the uniaxial strength of concrete. The dependence of material strength on the test method and on the boundary conditions is unacceptable and should be clarified.

A careful examination of several major aspects affecting the compressive strength of concrete has been carried out in order to confirm or disprove very basic commonly accepted concepts and provide new insights into the most important (major) parameters. This is done with great respect to the enormous amount of work that has been done on the subject over the years and contributed a lot with enthusiasm to uncover the different aspects of the complex issue of compressive strength, but leaving aside a few of them. This paper presents a modest attempt to contribute to clarifying a few aspects of the latter.

The research approach is based on a methodological examination of the entire issue, starting with the distinction between the common perception of a tested material having the specimen's shape, and the new evaluation of the specimen as a structural element responding to the applied compressive pressure. It examines the possible modes of damage/failure that may develop during loading and evaluates the relationship between the limit state behavior and the sought compressive strength. These findings lead to the paper insights and conclusions.

## 2 Behavior of the specimens and the material

### 2.1 The specimen's strength and material's strength

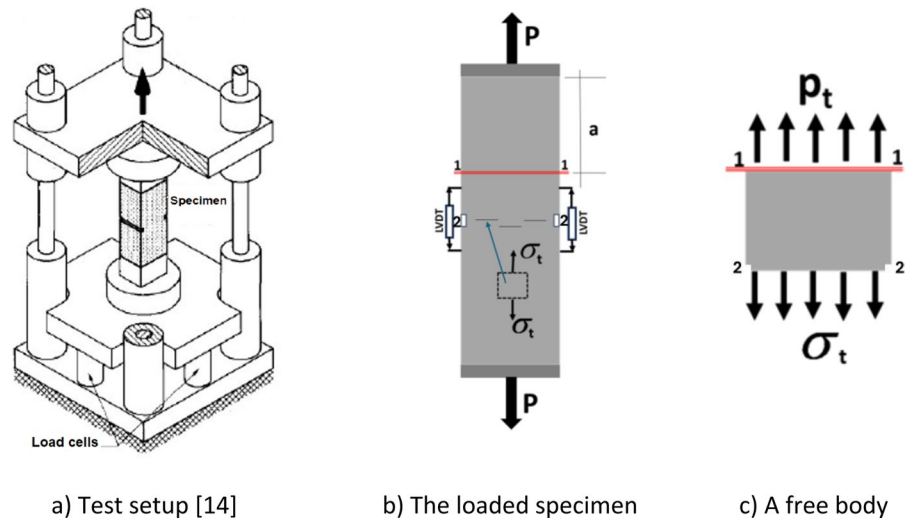
The uniaxial compressive strength of a given concrete material is determined from the maximum uniaxial compressive pressure loading resisted by a standard size specimen made from that concrete. That approach is based on an unconscious hidden conjecture that the maximum pressure applied on the specimen is equal to the maximum material compressive resistance, i.e. its strength. This conjecture has never been mentioned, nor proven. That issue has never been discussed explicitly because it seems so obvious and straightforward, and is considered as the common definition of the compressive strength. One may even wonder how else can one test the material compressive strength if not through loading a specimen made of that material up to its compressive failure?. This paper claims that the *pressure causing specimen failure* is not necessarily equal to the *concrete strength*. Elaboration of that issue opens new thoughts and yields new understanding of that fundamental issue. The relationship between the material's strength and the specimen's strength, should be analyzed separately and the linkage between the two should be unravelled.

As a first step, let us examine the uniaxial tensile test, which is a good example to demonstrate the tight relationship between the specimen's strength and the material's strength, where a planar crack of controlled width is developed perpendicularly to the loading axis direction. The relationship between the applied load and the crack extension is measured and the material tensile strength as well as the entire force–displacement relationship is determined.

### 2.2 The uniaxial tensile stress–strain behavior of concrete

Consider a uniaxial tensile test of a concrete specimen that is carried out under a displacement loading control protocol. A relatively  $150 \times 60 \times 50 \text{ mm}^3$  slender specimen, is prepared (Fig. 2a) [14], with saw cuts at mid-height producing small grooves at two opposite ends of the cross-sectional area. The saw cuts aim at creating a zone of a somewhat smaller cross-section area at the specimen mid height, thus ensuring development of higher tensile stresses at that specified zone



**Fig. 2** Uniaxial tensile test

and attempting to avoid stress concentration. Therefore, micro-cracks will develop in this zone during loading prior to any damage at any other cross-section along the specimen, and upon reaching the maximum load level corresponding to that early damage, a descending branch of the stress-displacement curve will follow and no damage will occur at any other cross-section along the specimen. With increasing tensile displacement, these micro-cracks will extend and coalesce into a full crack. The saw cuts zone is essential to control the crack location; this will allow precise beforehand installation of small displacement transducers to monitor the small displacement growth of the cracked zone. Displacement measurement is not required to determine the maximum tensile load, but is essential for monitoring the load–displacement relationship in the cracked zone.

Prior to testing, the specimen is glued to the loading platens at its top and bottom faces. At a first glance it seems to adversely affect the testing result similarly to the friction effect of the steel platens that is discussed above regarding the compression test. But in a second thought, it seems the best and simplest way to attach the specimen to the loading platens. In a specimen of low slenderness the friction at the compression specimen ends, or the restraint imposed by the glue at the top/bottom faces of the tensile specimen, would induce shear stresses along the specimen height and affect the stresses at the central zone of interest, but considering the present specimen high slenderness (Fig. 2) assures that the shear stresses at the end faces, which maintain

self-equilibrium at the contact face, will have no effect beyond a certain distance from the platens, thus the central part of the specimen will not be affected by that boundary condition.

Thus, the tensile loading  $P$  maintains equilibrium with an evenly distributed tensile stress  $p_t$  at a distant cross-section from the loading platen (1–1 in Fig. 2b, c), and with the evenly distributed tensile stress  $\sigma_t$  at the central cross-section (Fig. 2c).  $\sigma_t$  is slightly higher than  $p_t$  due to the slightly smaller cross-section area at the notched cross-section, and this triggers cracking at that cross-section. The maximum applied tensile stress determines the maximum tensile stress  $\sigma_t$  that is the cracking stress in a plane perpendicular to the loading axis. Therefore this maximum tensile stress determines the material tensile strength. This confirms that in this case the specimen strength is identical with material strength. It should be noted that this discussion focuses on the specimen and material strengths, and other considerations affecting the material strength, such as the size effect, are beyond the scope of this discussion.

The above discussion and conclusions are based on equilibrium considerations in the longitudinal direction. It cannot automatically reflect on the correctness of the force–displacement or stress–strain curves for uniaxial tension that are obtained using the LVDT displacement readings, and this aspect should be examined separately with caution. While concrete tensile strains may represent the concrete extensions during low magnitude loading, strain cannot represent the extensions across the cracked zone at a stage

where microcracking develops, and the LVLDT displacement reading over a short finite length (Fig. 2b) bridging the crack zone is the proper measure of the crack opening that is the displacement difference between the two LVDT ends. Another displacement measurement is the overall axial elongation between the specimen's platens. The latter is composed of two components: the integrated strains over the uncracked part of the measured span, and the concentrated extended displacement at the microcracked zone [15, 16]. Thus, the measured stress-displacement relationship depends on the LVDT span, and this is also the case for the stress-displacement relationship at the process zone. As its reading is also combined of these two components, the crack opening component that is required for the stress-displacement relationship, should be extracted from the original LVDT data [16] to provide a local stress-displacement behavior characteristic curve of the concrete in tension until cracking occurs.

In this uniaxial tensile test, the relationship between the maximum applied *tensile load*  $P$  and the *concrete tensile strength*  $\sigma_t$  is evident. It should be noted that the maximum tensile stress marks the beginning of the cross-section weakening, and the increase of the micro-cracking process. A softening branch begins at that stage along which the specimen tensile resistance drops to zero when a full crack across the specimen is formed. It should be noted that although this testing procedure seem simple, it requires careful and precise treatment [14].

This uniaxial tensile test demonstrates a case of excellent accordance between the specimen resistance and the material resistance. This is an exceptional example that is not indicative of other cases. The case of uniaxial compressive strength using a similar specimen and test setup, is entirely different as shown in the following.

### 2.3 Is a similar approach feasible for the compressive strength of concrete?

An attempt to extend the same procedure to determine the uniaxial compressive strength of concrete, is not straightforward, and different considerations that are presented below shed doubts whether extension of the same approach is justified and will yield the expected result.

A fresh, unprejudiced, independent thought on that matter leads to uncouple the *concrete specimen* from the *concrete material* and distinguish between the *applied uniaxial compressive pressure* that causes the specimen's failure and the *uniaxial compressive strength* of that concrete material associated with the material compression failure.

According to that way of thinking, the concrete specimen should be considered as a structural element that is made of concrete and is subjected to the longitudinal (uniaxial) compressive loading on its top and bottom faces. This structural element (the test specimen) responds to the applied compressive loads and internal stresses and strains are developed within the specimen to maintain equilibrium with the external loading until the structural element failure occurs. This is the way to look at a structural element in general, and at the specimen in our case in particular.

Following the logics outlined above regarding the uniaxial tensile test, in the case of uniaxial compressive loading, the test specimen may be considered appropriate to yield the concrete compressive strength only if the stress and strain fields within the specimen are of uniaxial compression as well, and that the specimen fails in uniaxial compression, in a plain that is perpendicular to the loading direction. While in the case of tensile loading, failure develops through cracking in a plane perpendicular to the load axis, in the case of compression, failure in compression cannot develop perpendicular to the load direction and it is unclear how does uniaxial compression failure looks like. If the above conditions cannot be fulfilled in the case of longitudinal compression loading, such uniaxial compressive failure mode can not occur hence a material compressive strength cannot be determined. The question now is how else the specimen may fail, and whether such failure may indicate about the compressive strength of concrete. A specimen structural element that is subjected to uniaxial compressive pressure, may develop different alternative modes of failure that maintain equilibrium with the applied loading that will be presented in the following. No matter what the failure mode of the specimen is, we should clarify that opposed to the common convention, the corresponding limit loading causing that failure cannot generally be considered the concrete material strength. This may be clarified by an analogy referring to a beam structural element, that is loaded by compressive loading and may fail





in bending or in shear. In each case a corresponding limit load maintains equilibrium with the developed failure mechanism and the support reactions, and considering the structural system geometry. In any of these modes the corresponding limit load cannot be considered as the beam material strength. It is only the load that maintains limit equilibrium corresponding to the failure mechanism.

This general thought of alternative failure modes of the loaded specimen is further elaborated in the following for the particular case of uniaxial compressive loading.

### 3 A specimen under a uniaxial compressive loading

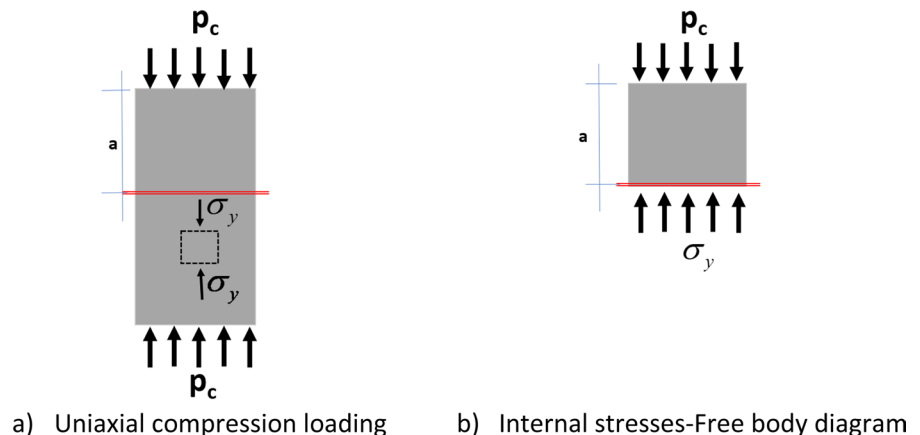
Consider a concrete specimen that is subjected to an external compressive evenly distributed applied pressure  $p_c$  acting in the longitudinal direction (Fig. 3a), similarly to the specimen loaded in tension in Fig. 2. A uniform uniaxial state of stress, that is equal to the applied compression  $p_c$  is developed. Corresponding axial compressive strains and lateral tensile strains due to Poisson's effect are developed. A free body diagram (Fig. 3b) depicts the interior uniaxial compressive stresses  $\sigma_y$  acting on the interior horizontal surfaces on an elementary unit cell in the tested specimen. The internal compressive stress  $\sigma_y$  in the axial direction can be determined from the exterior applied loading, similarly to the case of tensile loading (Fig. 2), i.e.,  $\sigma_y = p_c$ .

This describes the state of equilibrium for commonly used specimens of low or moderate

slenderness. For the sake of further understanding the difference between the structural response and the material's response, consider a non realistic specimen of high slenderness; upon increasing the compressive load magnitude, this specimen may reach a stage of instability and undergo sideway buckling under the applied centric compressive loading. At that instant the specimen responds like an elastic structural element in which the stress and strain fields, as well as its curvature, differ considerably from the previous uniform distribution of axial compressive stresses. Evidently, the critical compressive loading upon buckling is smaller than the maximum possible pressure that could be applied to a shorter specimen of the same cross-section and concrete type where buckling would not occur. Although that hypothetical mode of buckling failure cannot occur in low slenderness common specimens, this example aims at demonstrating that the evenly distributed compressive loading may maintain equilibrium with different modes of failure, and in the described scenario the central compressive load maintains equilibrium with either evenly distributed compressive stresses on an internal horizontal cross-section, or alternatively a linear variation of normal stresses that result from a superposition of the evenly distributed compressive stresses due to the axial load and linearly distributed compressive and tensile stresses due to the bending moment caused by the axial force couple upon the onset of buckling.

Return now to the low slenderness specimen that is commonly used for compression strength testing, and follow a further increase of the applied compressive loading  $p_c$ . The question is: what is the maximum load level that may be reached and how it is

**Fig. 3** A specimen under low magnitude uniaxial compressive loading



related to the compressive behavior of the material and to the developing damage. A maximum load level should refer to a limit state that is characterized by developing damage with increasing axial deformation provided by the loading apparatus and following failure, that are characterized by stiffness and resistance decrease with increasing deformation.

As mentioned above, crushing damage cannot occur on a horizontal plane (Fig. 3b) that is perpendicular to the compression loading axis. It seems that another limit state mechanism of the tested specimen should be reached at a certain stage of loading. Such limit state may occur due to another weakness of the tested element, and as such the maximum attained loading pressure is related to that specific weakness, that is not related to the compressive strength of concrete. The above discussion aims at clarifying that the *structural element strength under compressive loading*, may be entirely different from the *compressive strength of the material* from which the specimen is made of. The following section aims at examination of possible modes of structural element failure.

#### 4 Failure mechanisms of a structural cube element subjected to compressive loading

In this section we aim at examining possible failure mechanisms of a structural specimen element, that may determine limit states that correspond with a maximum applied compressive pressure. Two major possible damage and failure mechanisms will be presented.

##### 4.1 Lateral extension of a cube specimen loaded by a uniaxial longitudinal compressive pressure

Consider a homogeneous cubic specimen made of concrete that may be simulated by a linear-elastic model, characterized by its Young Modulus  $E$  and Poisson's ratio  $\nu$ . Applying an evenly distributed compressive pressure loading  $p_c$  on its top and bottom faces will produce compressive strains  $\varepsilon_z = \frac{p_c}{E}$  in the longitudinal direction  $z$  and tensile strains  $\varepsilon_x = \varepsilon_y = -\nu \frac{p_c}{E}$  in the lateral directions  $x, y$  (where  $p_c$  is assumed positive in compression). It turns out that the magnitude of  $p_c$  cannot exceed a loading level at which the tensile lateral strains reach the cracking strain limit  $\varepsilon_{\text{cracking}}$ , that is related to  $p_c$

through Poisson's ratio  $\nu$ . Evaluating common values of  $\varepsilon_{\text{cracking}}$ ,  $E$ ,  $\nu$ , yields the limit magnitude of  $p_c$  in that scenario, which is considerably smaller than the reported uniaxial compressive strength values that is obtained in common laboratory tests of specimens loaded by steel platens.

This mode of longitudinal cracking failure has been inspected in specimens loaded by steel platens using different friction reduction techniques at the specimen top and bottom faces. These techniques were reported as reducing the amount of friction, though not eliminating it completely. The magnitude of the applied pressure at the cracking limit state is considerably lower than the reference maximum pressure for specimens loaded using regular steel platens. The softening branch of the cracked specimens is smaller in comparison to the softening branch in the common case. In the ideal case of a perfectly smooth interface, longitudinal cracking appears and develop into longitudinal crack planes, perpendicular to the top and bottom loaded platens. These cracked planes split the specimen into longitudinal slices. A limited amount of friction on the specimens top and bottom faces somewhat distorts the ideal planar shape of these cracks [17, 18].

This may be observed in Fig. 4a where a single Teflon sheet is used for friction reduction of our tested cube. The friction shear effect is reflected by the cracks inclination, and the restraint to open more cracks upon increasing the longitudinal displacement along the softening branch. Implementing two layers of wax paper as a friction reduction interface produces vertical almost planar cracked surfaces (Fig. 4b). These cracks develop gradually during loading.



a) Teflon friction reduction b) Wax paper friction reduction

**Fig. 4** Longitudinal cracking dependence on friction reduction





At a high load level that approaches the peak loading and slightly afterward along the upper part of the softening branch, two early cracks develop (Fig. 5a). The widths of these cracks extend with increase of the longitudinal deformation. Then, two more cracks are developed along the softening branch (Fig. 5b). The width of these cracks extends as well with increasing deformation, and then, at a lower load level along the softening branch, another central crack opens (Fig. 5c). In an ideal homogenous specimen that is subjected to a uniform tensile strain across the specimen, any longitudinal plane may be cracked. In a real concrete specimen, the slight variation of the cracking strain and the flaws distribution activates a first plane cracking, after which very slightly further increasing longitudinal strain activates cracking in another plane and so forth.

This crack pattern is compared with almost ideally longitudinal cracked planes, in the case of friction reduction using wax paper (Fig. 4b).

Several observations demonstrate the difference between these two friction reduction methods:

- Cracked planes in Fig. 4b are longitudinal and almost planar, with local curvatures resulting from the aggregates texture and the formation of rough cracked surfaces as a result.

The interfacial friction in Fig. 4a restrains the opening of a minimal number of cracks the width of which extends along the softening branch. No more cracks are developed afterwards. This cracking mode is compared to the cracking evolution in Fig. 4b that refers to a smaller interfacial friction, and is characterized by an increasing number of cracks that are developed mainly along the softening branch (Fig. 5).

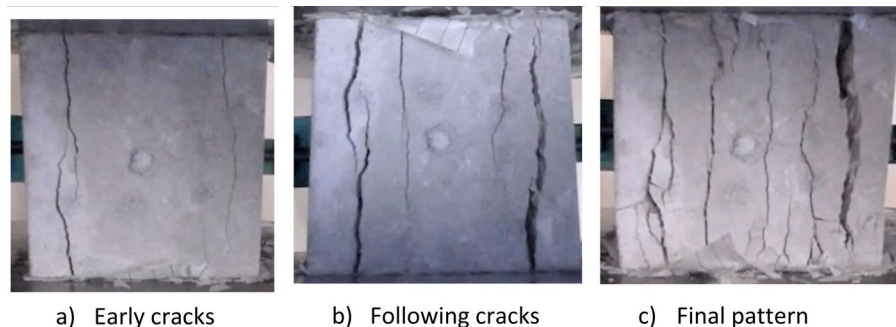
- The smaller the frictional stresses are, the steeper is the softening branch and the smaller is the maximum applied pressure at failure (Fig. 4b).
- The longitudinal concrete slices modify the initial shape of a low slenderness cube into a set of high slenderness slices. As such, each slice is considerably more sensitive to crack surface irregularities which influence the longitudinal applied load eccentricity, and its effect on possible buckling failure of such slices.

It may be summarized that although the specimen is subjected to compressive loading, the failure is due to tensile cracking occurring in longitudinal planes. Hence this failure is not related to the compressive behavior of the concrete material but rather to its tensile relative weakness.

Therefore, the recommended procedure for concrete specimens testing, using lubricated platens to allow determination of the complete stress–strain relationship with emphasis on the softening branch [13], turns out to yield the compression ascending branch up to the level at which longitudinal tensile cracks are developed. The following descending branch results from the further development of longitudinal tensile cracked planes, and further weakening of the specimen. It is not related to the concrete compressive behavior whatsoever, and certainly not exhibiting the compression strength.

The tensile cracking failure mechanism explains the steep softening branch measured in specimens loaded by friction reduced steel platens [17]. It is in accordance with the brittle nature of the tensile failure and the steep softening branch of the uniaxial stress–strain relationship in tension [14, 15]. Therefore the softening branch stands for the

**Fig. 5** Stages in tensile cracking development



tensile-cracking failure and the limited friction effect, that are not related to compression failure at all.

#### 4.2 Shear failure of a cube specimen subjected to uniaxial compressive loading

Let us return to the cube specimen that is subjected to uniaxial compressive loading, which is applied using lubricated platens. It has been shown experimentally that the mode of failure is that of longitudinal cracking. To extend the study on the compressive strength, assume now that the cracking strain/strength is sufficiently high such that the compression loading may exceed the maximum level attained earlier without activating the mode of lateral cracking that is discussed in Sect. 4.1, or that some lateral confinement provides that restraint. The question is: what is the following failure mode that will develop, requiring a higher applied pressure level?. As failure cannot develop along horizontal planes under normal compressive stresses only, and longitudinal cracking is not enabled, the state of limit equilibrium with the applied load (Fig. 3a) may be examined along an inclined plane (Fig. 6). In fact two mirror image states of equilibrium exist in the planar case. In each of them, for any given surface inclination  $\vartheta$ , the internal normal ( $N$ ) and shear ( $T$ ) forces maintain horizontal force equilibrium, and both together balance the longitudinal applied load provided by the distributed pressure on the top surface.

To analyze the equilibrium at that limit state of failure, a rigid plastic solution may be adopted. As elastic deformations are disregarded, the specimen will not fail in lateral tension and frictional stresses

will not appear on the specimen loaded faces due to relative lateral deformations of the specimen and the platens. This allows further increase of the applied compressive pressure until the following weak link (Fig. 6) is developed. That model enables further examination of the developing damage and investigate what is the maximum compressive load at that limit state.

The limit equilibrium is depicted on an interior inclined plane, at an angle  $\vartheta$  with respect to the horizontal axis (Fig. 6). The magnitudes of the normal compressive force  $N(\vartheta)$  and the tangential shear force  $T(\vartheta)$  depend on the magnitude of the applied force and on the angle  $\vartheta$ , and satisfy the equilibrium equations in both lateral and longitudinal directions. In fact, two twin surfaces exist, providing these equilibrium requirements, and therefore both are similarly possible. In the special case ( $\vartheta=0$ ) the general case (Fig. 6) coincides with the state of stress depicted in Fig. 7a. All states of stress are represented by points along the Mohr circles (Fig. 7b).

Figure 7a shows the stresses in the  $x,y$  directions acting on a differential volume element within the specimen. Several Mohr circles are depicted (Fig. 7b), representing increasing magnitudes of the applied pressure and the corresponding longitudinal compressive stress  $\sigma_y$  ( $\sigma_{y3} > \sigma_{y2} > \sigma_{y1}$ ). Transformation of the state of stress for the larger longitudinal stress  $\sigma_{y3}$  (point  $0_3$ ) is shown as points on the larger diameter Mohr circle. Point A describes this state of stress on a plane with an inclination angle  $\vartheta$ , subjected to the stresses  $(\sigma_A, \tau_A)$  acting on the rotated differential volume element. At a certain load magnitude ( $P_{c,max}$ ), sliding of the inclined surfaces occurs at an inclination angle  $\phi$ , which determines the failure of the loaded specimen (Fig. 8a).

Increasing the circle diameter is associated with increasing the magnitude of the shear stress  $\tau_A$ . Upon reaching the limit state, the Mohr circle become tangent to the shear failure envelope (lines I and II in Fig. 8a). The shear failure envelope is ideally described by the cohesion  $c$  and the angle of internal friction  $\phi$ . This envelope determines the maximum shear that the material can sustain on a plane with a given normal compressive stress, upon the occurrence of shear failure. Evidently this shear failure along inclined surfaces may equally develop in the two symmetrical directions (Fig. 8b).

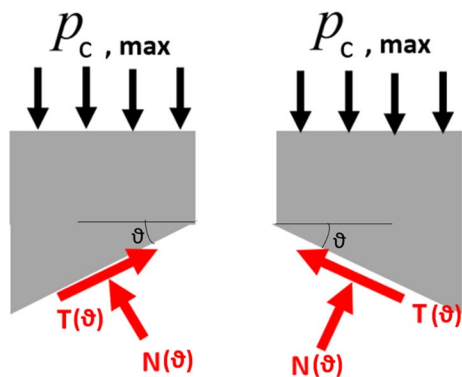


**Fig. 6** Twin free bodies at ultimate state



**Fig. 7** State of stress at a point in the specimen

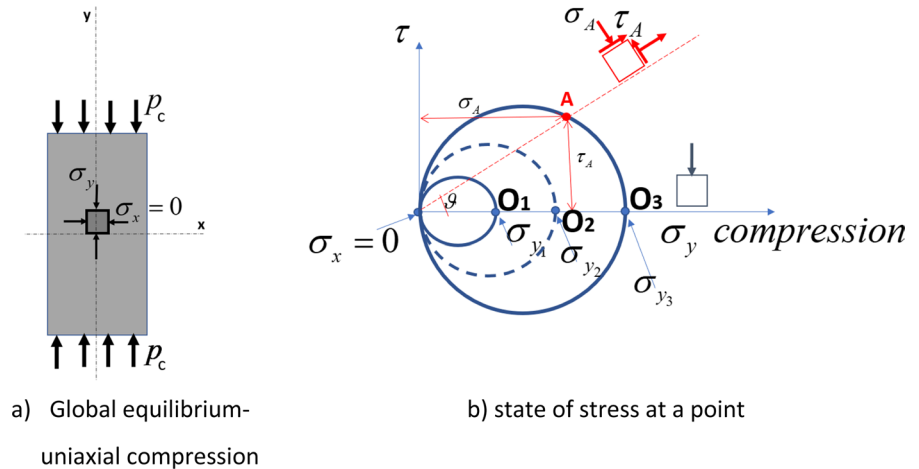


**Fig. 8** Mohr circle and shear planes

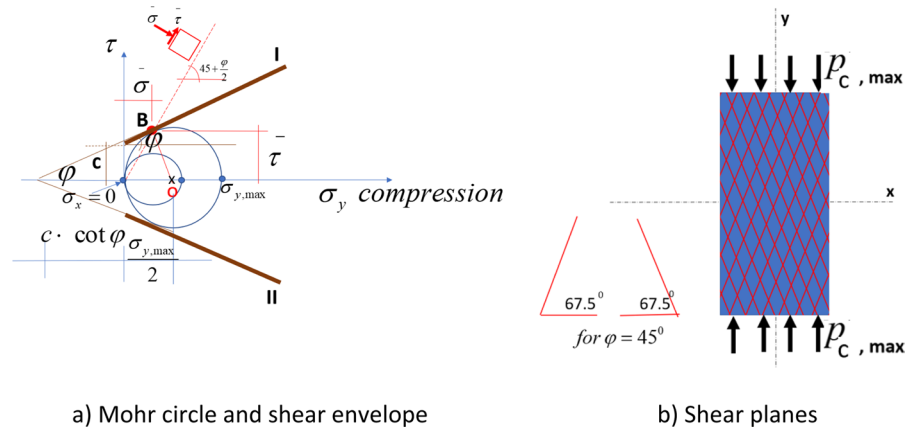


Figure 8a shows that point B on the failure envelope with coordinates  $(\bar{\sigma}; \bar{\tau})$  is tangent to a circle with a diameter  $\sigma_{y,max}$ . This is the largest possible stress circle prior to shear failure occurrence, with a diameter  $\sigma_{y,max}$  (that is equal to the maximum applied compressive pressure on the specimen top face). According to Fig. 8a, the stress coordinates of point B act on a plane that is rotated at an angle  $(45^\circ + \varphi/2)$ , that is the inclination angle of the shear plane at failure. A mirror failure condition with the shear envelope II (Fig. 8a), yields the mirror shear plane inclination. As Fig. 7a refers to a uniform uniaxial compression stress field, the shear planes at failure may develop at any location (Fig. 8b). The inclination of the failure planes is shown in Fig. 8b for a particular case where  $\varphi = 45^\circ$  and the failure planes inclination is therefore  $67.5^\circ$ . In the case where  $\varphi = 30^\circ$  the planes inclination is  $60^\circ$ , that is not much different.

Although a limit compressive pressure loading is reached, the formation of these shear planes within the specimen are not related to the compressive behavior of the concrete material whatsoever, but to the formation of shear planes in the specimen. This mode of shear failure is similar to the common failure inspected in cube or cylindrical specimen testing, and the maximum compressive pressure loading associated with that failure is commonly wrongly defined as the compressive strength of concrete.

It should be noted that the infinite number of potential failure planes results from the assumed homogeneity of the specimen domain. The real specimen however, is heterogenous and contains numerous aggregate inclusions. Therefore it is reasonable to assume that a limited number of planes of least resistance will develop and govern the loaded specimen

failure. In fact, even the formation of a single failure plane satisfies the limit state condition.

From the geometry in Fig. 8a, the expression for the maximum uniaxial compressive pressure loading at the state of the specimen shear failure is:

$$p_{c,\max} = 2c \cdot \frac{\cos \varphi}{1 - \sin \varphi} \quad (1)$$

Equation (1) shows that the maximum applied pressure at that limit state depends on the cohesion and the angle of internal friction ( $c$ ,  $\phi$ ), that are the shear envelope parameters. Hence, the maximum applied pressure is related to the shear failure and is not related to the compressive failure of concrete, whatever it is. Moreover, Eq. (1) demonstrates that  $p_{c,\max}$  is not a material property. A material property is a prime value that cannot be calculated from other prime properties, and therefore it should be measured by standard test methods, dedicated to measure that specific property (e.g., Young's Modulus, Poisson's Ratio). Hence, Eq. (1) is a function of material properties and it can be calculated from the  $c$ ,  $\phi$  data.

## 5 Shear planes in standard concrete cube tests under uniaxial compressive loading

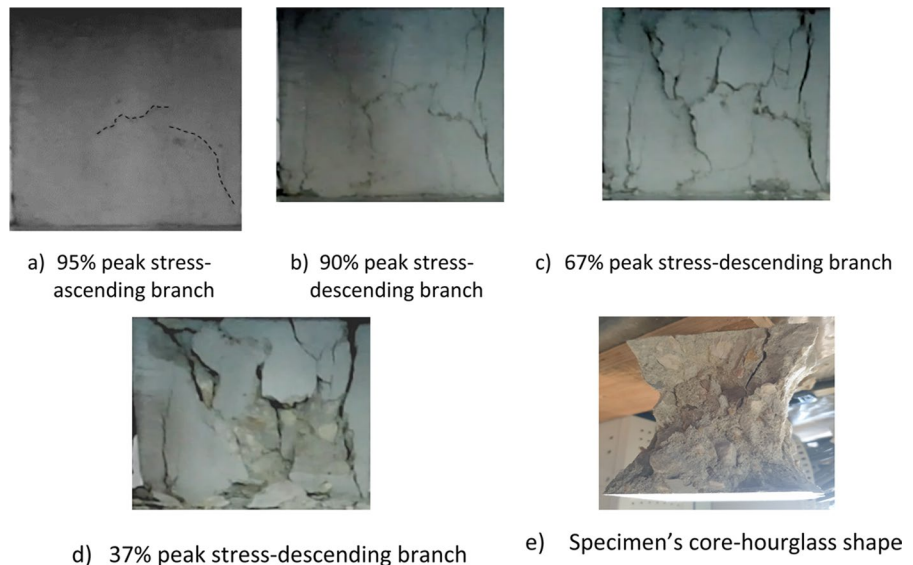
Standard 100 mm sided cubes had been prepared (Table 1) and were tested to uniaxial compressive loading. The average compressive pressure (commonly assumed as the compressive strength of the concrete) from six specimens was 32.2 MPa. More specimens were tested to monitor the damage development during loading increase. An almost linear ascending branch is observed up to 90–95% of the peak load. Close to the peak load early local minor signs of damage are observed (Fig. 9a). Beyond the peak load, the damage is growing, and the number of cracks, their width and length expand considerably; the damage expansion is accompanied by a sharp descent of the load that corresponds with the increasing measured displacement.

Figure 9b shows the damage on the cube front face along the descending branch where the load decreased to 90% of the peak load. Upon further longitudinal displacement, where the load magnitude

**Table 1** Concrete composition (per 1 m<sup>3</sup> concrete)

Cement CEM I 52.5	Water	Additive G-100-X	Water/ cement ratio	Coarse aggregate	Fine aggregate	Natural sand
Kg 253	Kg 200	Kg 1.52		Kg 770	Kg 378	Kg 715

**Fig. 9** Damage evolution in a specimen during a standard test



decreased to 67% of the peak load, a final cracking pattern has been shaped (Fig. 9c) and further displacement shows spalling of concrete parts and their detachment from the specimen core (Fig. 9d). Upon reaching an almost zero specimen's resistance and after removal of loose concrete parts, the specimen's core having an hourglass shape is exposed (Fig. 9e).

Figure 10a, c present the hourglass shapes of two specimens after their complete failure. The inclined shear planes are clearly observed. As the angle of internal friction of this type of concrete is unknown an average value of  $\varphi = 35^\circ$  is assumed to depict the inclination of the failure planes. Figure 10b, d show the calculated inclination of the shear planes (in red). Good correspondence with the slopes of the shear planes are observed.

## 6 Comparison with numerical results

Vonk [19] investigated the structural behavior of a concrete specimen, subjected to uniaxial compression loading, along the softening branch. Using finite element analysis including fracture mechanics, Vonk analysed the heterogenous specimens at the meso-level considering the aggregates and cracks in the

hardened cement paste. Aggregates were distributed randomly in the specimen domain.

To examine the influence of the random generation of the composite specimen, the same set of parameters was used to generate two specimens (T1 and M2) which were loaded in one direction, and two more simulations using the above specimens which were loaded in the lateral direction. To simulate the frictional restraint, two loading platens were modelled together with the specimen. Comparing the four simulations showed identical behavior along the ascending branch reaching the same peak load. The difference is observed in somewhat different descending branches accompanied by different lateral deformations at equal axial deformations and different cracking shapes. Figure 11 presents the different calculated cracking patterns of the four numerical specimens which split up into pieces with entirely different shapes and sizes. A major part of the shear planes is aligned in two clear inclination directions and a comparison with the above analysis of the idealized shear failure planes inclinations (in red) shows very good correspondence. Close examination of the different cases in Fig. 11, shows the clear effect of the coarse aggregates which force the developing cracks to circumvent aggregates along their path.



**Fig. 10** Comparison with test results

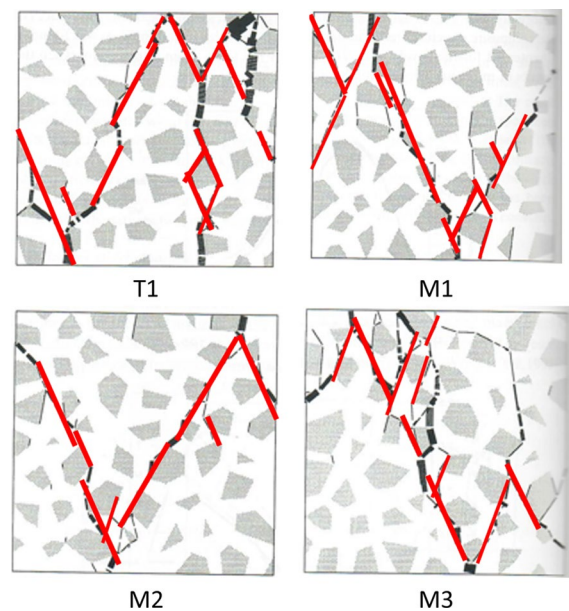


**Fig. 11** Comparison with numerical meso scale analysis



## 7 Calculation of the maximum applied compressive pressure

The maximum compressive pressure that yields shear failure of a standard cubical concrete body is considered in the following. It is erroneously considered as the uniaxial compressive strength of the tested concrete and incorrectly referred as a material property to which other strength parameters are related. The inclination of the theoretically calculated shear planes has been compared with experimental and numerical shear planes directions and excellent qualitative agreement has been shown above. This section aims at calculating the magnitude of the maximum compressive pressure at the shear failure limit state and demonstrate the quantitative excellent agreement with the measured compressive strength of the cube specimen. It will show that the maximum compressive pressure may be calculated from basic material properties, hence demonstrating that the magnitude of the compressive loading at the limit state, is not a material property, and it is not a measure of the uniaxial compressive strength of the concrete material.

Consider the shear planes failure mechanism that is developed under the action of the compressive pressure loading  $p_{c,\max}$  as shown in Fig. 8. Equation (1) expresses the maximum applied pressure  $p_{c,\max}$  at that limit state, using the cohesion  $c$  and the angle of internal friction  $\phi$ . In fact,  $p_{c,\max}$  in the rigid body model may be somewhat different from that in the real case, where the pressure is transferred to the specimen through the platen. However, due to the similarity of the real shear planes configuration (Figs. 10, 11) and the idealized planes orientation (Fig. 8), close values of the measured and calculated  $p_{c,\max}$  are expected.

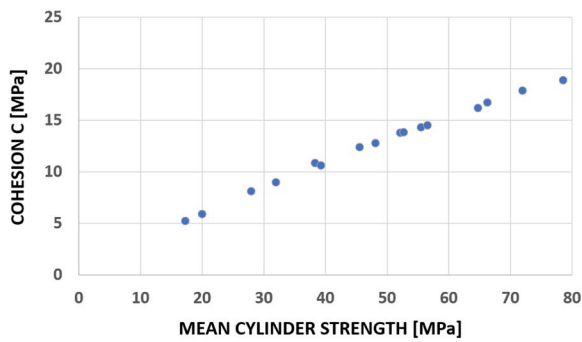
To calculate the magnitude of  $p_{c,\max}$ , the values of  $c, \phi$  are required. In earlier studies related to projectile penetration into concrete targets, Yankelevsky [20] found that the so called uniaxial compressive strength of concrete, cannot identify a specific type of concrete and determine the target resistance. It was proven that concrete targets made from equal uniaxial concrete strength (according to the common convention) but from different mix compositions, performed differently and exhibited different resistance and damage characteristics [22]. Nevertheless, the concrete strength still plays the central role in concrete mechanics and all parameters including  $c, \phi$  are given in the literature as function of the concrete

compressive strength, only because it is traditionally considered as the key and only characteristic parameter of the concrete. This fact raises up an apparent dilemma: the  $c, \phi$  data is given in the literature as function of the uniaxial compressive strength, and here we want to predict the compressive strength from Eq. (1) based on the related  $c, \phi$  parameters. However, the wider the range of concrete strengths is, that are made from different mixes, the compressive strength is just a ruler to present the continuous relationships of  $c, \phi$  and the concrete that is represented by a strength parameter. We refer to an investigation aiming at determination of the parameters of the Drucker-Prager yield criterion, and for that purpose an experimental program has been carried out to determine the  $c, \phi$  values for 16 different mixtures covering a wide range of NSC and HSC concrete types and two different maximum coarse aggregate sizes [21]. Triaxial compression tests were carried out on cylindrical specimens. Several tests were performed for a given concrete type; in each test a different lateral confining pressure level was applied as the minor principal stress and the axial pressure was then increased until failure was reached and determined the major principal stress at failure. These principal stresses determine Mohr's circle diameter at failure. Having several circles relating to different sets of minor/major principal stresses, allows to plot the shear failure envelope, which is common to all these circles and experimentally yields the values of  $c, \phi$ . To refer to the obtained cohesion and angle of internal friction values, strength of each concrete type was determined from standard 150 mm sided cubes, also in addition to its determination through using the same cylinders for the special case of zero lateral pressure, thus applying a uniaxial compressive pressure on cylinders that are similar to those tested under triaxial conditions. In the following we refer to the mean cylinder uniaxial concrete strength to avoid the need of converting the tested cube strength to the cylinder strength considering the variable conversion due to the wide strength range, the differences in shape and size, and to eliminate the discussion of the platens friction effect on the conversion.

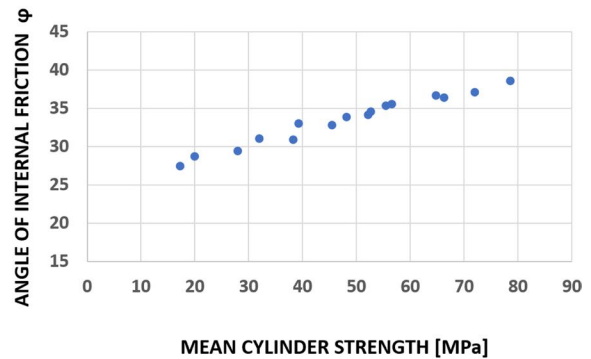
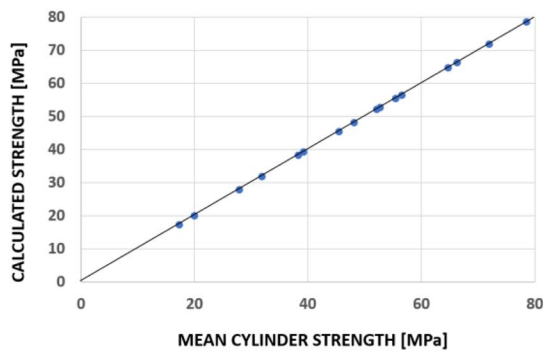
Figure 12a describes the variation of the experimentally determined cohesion over a wide strengths range. An excellent fit with a linear correlation coefficient of  $R^2 = 0.995$  is obtained.



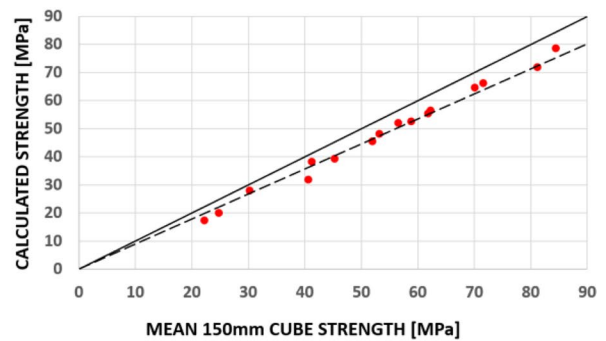




a) Variation of cohesion

b) Variation of  $\phi$ 

c) calculated/measured cylinder strength



d) calculated/measured cube strength

**Fig. 12** Shear failure strength prediction

Figure 12b describes the variation of the experimentally determined angle of internal friction over the same strength range. An excellent fit with a linear correlation coefficient of  $R^2 = 0.972$  is obtained.

Using these values of  $c, \phi$ , the maximum compressive pressure loading at shear failure ( $p_{c,max}$ ) has been calculated from Eq. (1). Figure 12c compares the calculated value of  $p_{c,max}$  with the reported uniaxial compressive strength of the cylindrical specimens, as measured in the triaxial apparatus. All the calculated results are laid along a 1:1 solid line, indicating a perfect fit. It means that using Eq. (1) and the  $c, \phi$  data,  $p_{c,max}$  is predicted at excellent accuracy. Comparison of the calculated value of  $p_{c,max}$  with the reported compressive strength of 150 mm sided cubes is shown in Fig. 12d. All calculated points are placed along the linear dotted line indicating a ~10% lower

magnitude than the values in Fig. 12c. That difference is attributed to the size effect mentioned above.

This comparison demonstrates the strong correlation between the cohesion and the angle of internal friction, which govern the limit pressure applied on a cube specimen causing shear failure. That confirms that the applied longitudinal pressure on the cube is related to the shear failure of the specimen. It instructs that the maximum measured loading, that is wrongly denoted as the compressive strength, is tightly related to the shear failure parameters  $c$  and  $\phi$ , that are considered material properties. These material properties vary depending on the concrete composition. The above analysis demonstrates that  $p_{c,max}$  is obtained from these shear envelope parameters. Therefore  $p_{c,max}$  is not a prime value but depends on prime material properties  $c$  and  $\phi$ .

## 8 On the very nature of concrete compressive strength

### 8.1 Summary and discussion

The behavior of a concrete specimen that is subjected to a uniform compressive pressure is characterized by an almost linear uniaxial stress–strain relationship until approaching a peak pressure.. Such an almost linear relationship stands for the undamaged behavior of the specimen under uniaxial compression.

Any further load increment, just before the stress peak or further strain increment beyond the strain corresponding to the peak stress is accompanied by damage development within the concrete material. It has been shown that the damage is either due to lateral tensile cracking or due to the development of inclined shear bands. The compressive pressure levels corresponding to either of these modes of damage are interpreted as the loads that maintain limit equilibrium with the developed damage mechanism of the specimen structural element, but cannot be related to a material property, or considered as the compressive strength of the concrete material. Upon reaching the limit state of any of these failure modes, it gains control on the continuing specimen response, and the compressive response cannot be followed further.

Therefore the peak load is not related to the compressive resistance of concrete, but to either the cracking or shear modes of failure, and referring to that maximum pressure level as representing the compressive strength of concrete is basically incorrect.

Experiments have shown that the frictional restraint between the platens and the specimen has a considerable effect on the peak loading and on the shape of the softening part of the stress–strain relationship [18]. Hence, the measured maximum pressure is significantly affected by the testing conditions. This blurs the significance of the measured values even for that purpose.

A RILEM TC 148-SCC document [13] provides guidelines for a standard test method to measure the strain softening behavior, where special care is given to reduce the friction between the platens and the specimen, thus leading to a relatively lower magnitude of the peak load. This leads to a tensile cracking mode at a relatively low pressure, compared to the limit pressure causing shear failure, which cannot provide the requested compressive strength of concrete.

The maximum pressure causing shear failure of a concrete specimen is a result of the limit shear equilibrium and depends on the fundamental properties of the shear envelope  $c$  and  $\phi$ . Since it depends on the prime properties of  $c$  and  $\phi$ , the maximum pressure associated with that shear failure is not a material property, and obviously it is not related to the compressive strength of concrete.

This means that the so called “compressive strength of concrete” represents the non slender *cube strength in shear* and not the *compressive strength of concrete*. It may be used as a reference value for describing and comparing different concrete types or for control of cast concrete quality in a project, however it cannot provide the constitutive behavior parameters of concrete in compression for structural analysis purposes nor the compressive strength of this concrete.

So, what is the compressive strength of concrete?

Consider three configurations of compressive loading of a cylindrical specimen:

- (a) uniaxial pressure loading on top and bottom faces of the specimen in the longitudinal direction;
- (b) same as “a”+evenly distributed radial pressure (in the lateral direction) over the cylindrical envelope, at a magnitude that is smaller than the axial pressure;
- (c) isotropic loading, where the radial pressure is of equal magnitude to the axial pressure loading.

In case “a”, which is the subject matter of the present manuscript, it has been shown that upon reaching a certain level of axial pressure a cracking or shear modes of failure develop, depending on the existence of friction with the steel platens, and the loaded specimen fails in one of these modes. Therefore, the axial loading cannot lead to a uniaxial failure mode in compression. That means that the *uniaxial compressive strength of the concrete material* does not exist at all, and the discussion should focus on the state of uniaxial pressure loading causing one of these modes of failure. It is important to emphasize that a real uniaxial compressive failure along the above criteria has never been reported. Moreover, it has been shown that specimen loading using lubricated platens activates the lower level pressure mode of longitudinal cracking, and prevention of this mode of failure allows further increase of compression resistance



until the higher level pressure that is associated with shear failure is activated. This indicates that compressive resistance may be further increase. This can be achieved in the case of a higher cracking strain/stress. This may also be achieved if lateral extensions are restrained, however adding that condition classifies the problem within case “b” or “c”.

In case “b”, the applied radial pressure opposes the weakness exhibited by the formation of radial cracks and allows increasing the axial pressure to a higher level, until shear band failure will occur. The higher the radial pressure is, the smaller the diameter of Mohr’s circle is, and higher compressive pressures can be applied without causing specimen’s failure. This can be clearly described in a smaller Mohr’s circle, with a diameter that is equal to the difference between the two applied pressures, and its center is shifted towards the right, thus positioned at a greater distance from the shear failure envelope. Fixing a certain level of radial pressure allows increase of the longitudinal pressure, until the condition of shear failure is fulfilled. That means that qualitatively, case “b” is not different from case “a”, and it is just the magnitude of the applied pressure that increases. Therefore, in case “b” no uniaxial compressive failure is developed as well.

In case “c”, all the principal stresses are equal, and the Mohr’s circle representing this state of stresses shrinks to a point on the axial stress axis. Hence shear failure cannot develop at any level of applied pressure and compressive failure cannot develop as well.

That means that compressive strength of the concrete material is a fictitious term. Concrete failure under compression will not occur even under extremely high isotropic compression loading. Experimental investigations on the behavior of concrete specimens under hydrostatic compression loading indicate that the specimen volume is decreasing with increasing pressure, however it is not reaching failure even under extremely high pressures [22]. The specimen response to hydrostatic compression exhibits increasing stiffness and bulk strain with increase of the applied compression. The increasing stiffness testifies that no failure is involved and the increasing volumetric strain results from compressibility of the micro pores in the hardened concrete. That means that there is no compression failure of concrete to which a “compressive strength” of concrete may be assigned.

## 9 Conclusions

These insights indicate that concrete is not reaching compression failure, and therefore the *compressive strength of concrete* is a fictitious term that has no physical meaning. Under an increasing applied compressive pressure along the ascending branch, the concrete material is reaching a stage of weakness where longitudinal cracking or inclined shear bands modes of damage are developed. At that stage, the response shifts into the particular mode of damage. Beyond the damage onset of any of these modes, the compressive response is not developing any further and cannot reach a state of compressive strength. This new understanding requires a new thinking regarding the definition of material strength and methods for its testing. It also requires to set limits on the stress–strain relationship of concrete in under compressive loading, and define its transition to the appropriate mode of damage/failure. Following the above insights it turns out that uniaxial stress–strain of concrete in compression may be followed only along the ascending branch prior to any damage indication of a mode of failure, after which the appropriate failure analysis should be followed. The beyond the linear ascending branch, the commonly used curve towards the peak zone and especially along the post peak descending branch (Fig. 1) is not representing the compressive behavior of concrete. Further elaboration of these issues is beyond the scope of the present paper.

Finally, a tribute is given to Prof. Adam Neville. In some way this paper echoes his ambiguous though important statement on the compressive strength of concrete given in his classical manuscript [23]: “we should be wary of interpreting it as a true measure of the compressive strength of concrete.” This paper aims at removing some of the ambiguity and call for re-thinking on concrete material response to compressive stresses, considering the stress–strain relationships representing the concrete material behavior under compression. This is a fundamental need that is essential for any concrete analysis and simulation.

**Acknowledgements** The authors extends thanks and appreciation to Dr. Y. Karinski, Eng. E. Itzhak and Mr. E. Gershengoren for their dedicated experimental work and technical support.



**Funding** Open access funding provided by Technion - Israel Institute of Technology.

**Open Access** This article is licensed under a Creative Commons Attribution 4.0 International License, which permits use, sharing, adaptation, distribution and reproduction in any medium or format, as long as you give appropriate credit to the original author(s) and the source, provide a link to the Creative Commons licence, and indicate if changes were made. The images or other third party material in this article are included in the article's Creative Commons licence, unless indicated otherwise in a credit line to the material. If material is not included in the article's Creative Commons licence and your intended use is not permitted by statutory regulation or exceeds the permitted use, you will need to obtain permission directly from the copyright holder. To view a copy of this licence, visit <http://creativecommons.org/licenses/by/4.0/>.

## References

- Park R, Paulay T (1975) Reinforced concrete structures. Wiley, Hoboken, p 763
- Nawy EG (2009) Reinforced concrete-A fundamental approach, 6th edn. Pearson Prentice Hall, Hoboken, p 914
- EC2 (2004) Eurocode 2: design of concrete structures—Part 1–1: General rules and rules for buildings
- ACI 318 (2014) 318–14: Building code requirements for structural concrete and commentary
- CAN/CSA-A23.3–04 (2004) A National standard of Canada. A23.3–04 Design of concrete structures
- fib-federation internationale du beton (2013) fib Model Code for Concrete Structures 2010. Wiley, New Jersey, p 402
- ASTM, C39 / C39M–18 (2018) Standard test method for compressive strength of cylindrical concrete specimens, ASTM International, West Conshohocken, PA
- European standard EN 12390–3 (2019) Testing Hardened Concrete—Part 3: Compressive strength of test specimens, European committee for standardization, June
- Van Mier JGM (1984) Strain Softening of concrete under multiaxial loading conditions, PhD thesis, Eindhoven University of Technology, The Netherlands
- Van Vliet MRA, Van Mier JGM (1996) Experimental investigation of concrete: fracture under uniaxial compression. *Mech Coh Frict Mater* 1:115–127
- Van Mier JGM, Shah SP et al (1997) Strain softening of concrete in uniaxial compression. *Mater Struct* 30:195–209
- Van Mier, JGM (1998) Failure of concrete under uniaxial compression: an overview, *Proceeding Framcos-3*, Aedificatio Publishers, D-79104 Germany, pp. 1169–1182
- Rilem TC (2000) 148-SSC: Strain softening of concrete—test method for compressive softening. *Mater struct* 33(6):347–351
- Hordijk DA (1991) Local approach to fatigue of concrete, Ph.D. Thesis, Delft University of Technology, The Netherlands, p. 210
- Yankelevsky DZ, Reinhardt HW (1989) Uniaxial behavior of concrete in cyclic tension. *ASCE J Structural Eng* 115(1):99–106
- Yankelevsky DZ, Reinhardt HW (1987) Response of plain concrete to cyclic tension. *ACI Mater J* 84(5):365–373
- Van Vliet MRA, Van Mier JG (1995) Softening behavior of concrete under uniaxial compression, *Proceeding Framcos-2*, AEDIFICATIO Publishers, D-79104 Freiburg, Germany, pp. 383–396
- Kotsovos MD (1983) Effect of testing techniques on the post ultimate behavior of concrete in compression. *Mater Struct* 16:3–12
- Vonk R. (1992) Softening of concrete loaded in compression, Ph.D. Dissertation, Eindhoven University of Technology, The Netherlands
- Yankelevsky DZ (2017) Resistance of a concrete target to penetration of a rigid projectile-revisited. *Int J Impact Eng* 106:30–43
- Öztekem E, Pul S, Hüsem M (2016) Experimental determination of Drucker-Prager yield criterion parameters for normal and high strength concretes under triaxial compression. *Constr Build Mater* 112:725–732
- Yankelevsky DZ, Karinski YS, Zhutovsky S, Feldgun VR (2023) Isotropic triaxial tests of equal strength concrete with different mix compositions. *Constr Build Mater* 408(133717):1–13
- Neville AM (1963) *Properties of Concrete*, 5th edn. Pearson Education, London, p 872

**Publisher's Note** Springer Nature remains neutral with regard to jurisdictional claims in published maps and institutional affiliations.

